



Get Clarity On Generics

Cost-Effective CT & MRI Contrast Agents



FRESENIUS
KABI

WATCH VIDEO

AJNR

Sequential MR Imaging Changes in Nonketotic Hyperglycinemia

J. Mourmans, C.B.L.M. Majoie, P.G. Barth, M. Duran, E.M. Akkerman and B.T. Poll-The

AJNR Am J Neuroradiol 2006, 27 (1) 208-211

<http://www.ajnr.org/content/27/1/208>

This information is current as
of August 9, 2025.

CASE REPORT

J. Mourmans
C.B.L.M. Majoie
P.G. Barth
M. Duran
E.M. Akkerman
B.T. Poll-The

Sequential MR Imaging Changes in Nonketotic Hyperglycinemia

SUMMARY: Serial diffusion-weighted (DWI) and diffusion tensor imaging (DTI) were performed in a patient with neonatal onset nonketotic hyperglycinemia (NKH). At 3 weeks areas that are normally myelinated at this time showed increased T2-signal intensity and restricted diffusion, consistent with vacuolating myelinopathy. At 3 months, these areas had increased in the topographic pattern of normal myelination, whereas fractional anisotropy was compatible with axonal sparing. At 17 months, diffusion restriction had disappeared, likely because of coalescence of myelin vacuoles. A decrease of fractional anisotropy was observed in the previously myelinated areas indicative of axonal loss. We conclude that DWI and DTI can be used to identify and characterize white matter tract abnormalities in patients with NKH.

Nonketotic hyperglycinemia (NKH) is a disorder of glycine metabolism caused by a defect in the glycine cleavage enzyme system, resulting in high glycine concentrations in urine, plasma, and especially CSF and the brain.¹ The diagnosis can be confirmed by enzyme assay in liver tissue or by mutational analysis.² Glycine plays 2 important roles in the central nervous system: an inhibitory neurotransmitter in the spinal cord and a modulator of excitation at the *N*-methyl-D-aspartate receptors in cerebral cortex, hippocampus, and cerebellum. In neonatal-onset NKH, neonates manifest lethargy, hypotonia, apnea, and intractable epileptic seizures. Probably because of the rarity of NKH, reports on the imaging findings are scarce. The outcome of conventional T2-weighted images in 7 patients from 4 days to 38 months old reflected supra- and infratentorial volume loss, impaired myelination of supratentorial tracts, but normal myelination in the brain stem and cerebellum.³ Two recent case reports described abnormalities of diffusion-weighted imaging (DWI) with restricted diffusion.^{4,5} High-signal-intensity DWI together with low apparent diffusion coefficient (ADC) probably reflect the well-known neuropathologic finding of vacuolating myelinopathy in NKH.

We report initial and follow-up MR imaging in a boy with NKH until death at 17 months, by using conventional imaging, DWI, and ADC, as well as diffusion tensor imaging (DTI). Using DTI as an additional instrument affords a means to study the progressive effect of glycine encephalopathy on axonal integrity in the affected areas.

Case Report

The male patient was born at term after an uncomplicated pregnancy and delivery. Apgar scores were 9 and 10, birth weight 4100 g, and head circumference 35 cm. On the fourth day of life, he was admitted because of progressive weakness and feeding difficulties. At the age of 16 days, myoclonic seizures were observed. Electroencephalography showed a burst suppression pattern, later evolving to an abnormal high voltage background pattern with frequent multifocal

epileptic bursts. The diagnosis of NKH was based on gross elevation of glycine in plasma (903 $\mu\text{mol/L}$; controls, 20–356 $\mu\text{mol/L}$) and in CSF (142 $\mu\text{mol/L}$; controls, 3–8.3 $\mu\text{mol/L}$), with an elevated glycine CSF-to-plasma ratio of 0.16 (normal < 0.02). The activity of the glycine cleavage system in biopsied liver tissue was clearly diminished (1.7 nkat/kg protein, controls 110 ± 41). Treatment with sodium benzoate (300 mg/kg/day) and dextromethorphan (3.5 mg/kg/day) decreased plasma glycine concentrations, but CSF glycine values remained unchanged. Only a temporary positive effect on seizure frequency and hypotonia was observed, despite increase of dextromethorphan to 10 mg/kg/day. Treatment with phenobarbitone and clonazepam had no effect on the epileptic seizures. Severe hypotonia, therapy-resistant epilepsy and developmental failure marked the subsequent course, and he died of respiratory insufficiency at the age of 17 months. Permission for autopsy was declined.

MR imaging of the brain was performed on week 3 and at 3 and 17 months, on a 1.5T unit by using a standard quadrature head coil. Conventional spin-echo T1-weighted 570/14 ms (TR/TE) and fast spin-echo T2-weighted 3500/22–90 ms (TR/TE_{eff}) images were obtained with an echo train length of 10, a field of view of 23×23 cm, an imaging matrix of 256×256 , a 5-mm section thickness with a 1-mm gap. Diffusion-weighted MR images were acquired with a field of view of 26×26 cm. Section thickness, gap, orientation, and section positions were the same as in the axial T1- and T2-weighted sequences. We used a single-shot, spin-echo, echo-planar (EPI) sequence, with a TE of 100 milliseconds, an acquisition matrix of 96×200 , reconstructed to 256×256 images. One image with a *b* value of 0 was acquired, and 6 images with *b* values of 1000 seconds/ mm^2 , with the diffusion sensitizing gradient pointing in 6 noncollinear directions, so as to gather complete diffusion tensor data. The repetition time between EPI-acquisitions was 4000 milliseconds. From the acquired data, the average ADC was calculated, namely, one third of the trace of the diffusion tensor, and the fractional anisotropy.⁶

The first MR imaging scan, at 3 weeks, showed a normal cortical gyration, corpus callosum, ventricular system, and cerebellum. On the T1- and T2-weighted images, the appearance of the white matter myelination was inappropriate for age. The axial T1-weighted images showed intermediate signal intensity in the dorsal brain stem, the middle cerebellar peduncles, the posterior limbs of the internal capsules, and bilateral corona radiata. On T2-weighted images increased signal intensity was found in the dorsal brain stem, the cerebellar vermis, the posterior limbs of the internal capsules, central corona radiata, and periolandic gyri (Fig 1A). DWI revealed hyperintense signal intensity in these areas (Fig 1B) in combination with low ADC

Received October 26, 2004; accepted after revision January 31, 2005.

From the Departments of Pediatric Neurology, Emma Children's Hospital (J.M., P.G.B., B.T.P.T.) and Radiology (C.B.L.M.M., E.M.A.) and the Laboratory of Genetic Metabolic Diseases (M.D.), Academic Medical Center, University of Amsterdam, Amsterdam, the Netherlands.

Address correspondence to: Professor B.T. Poll-The, Department of Pediatric Neurology (G8-211), Academic Medical Center, Emma Children's Hospital, Meibergdreef 9, P.O. Box 22660, 1100 DD Amsterdam, the Netherlands.

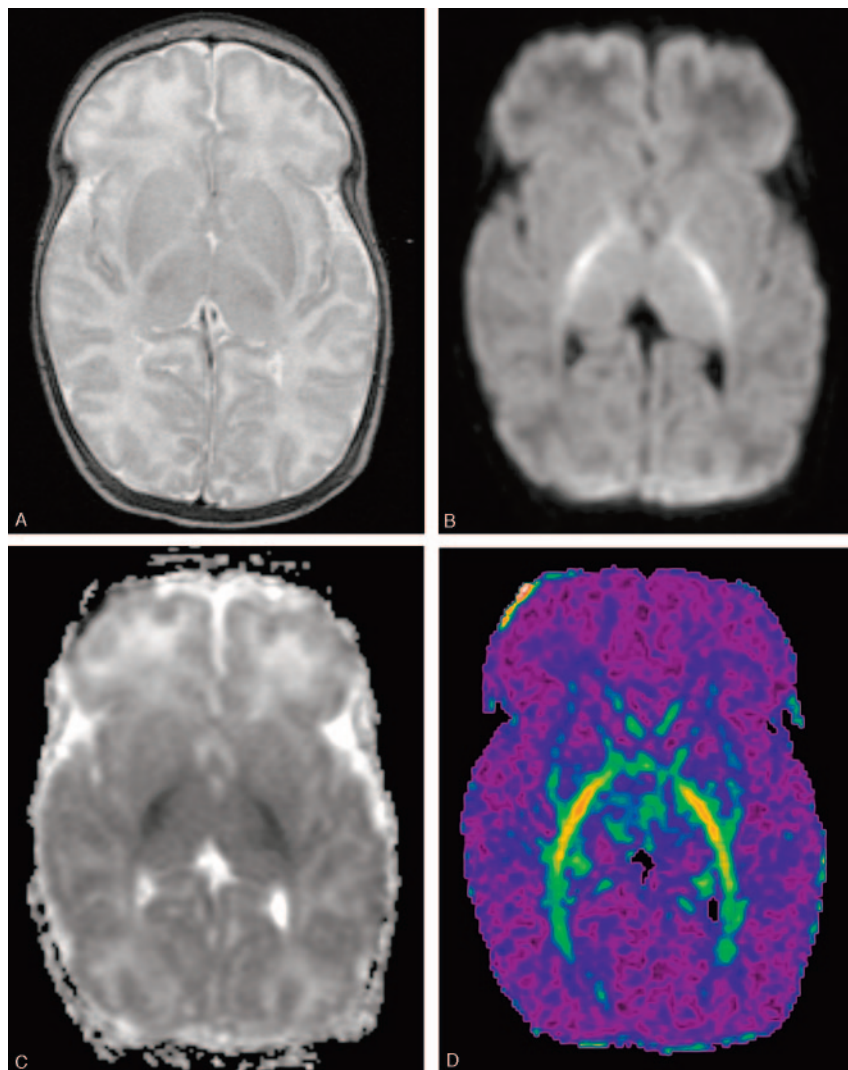


Fig 1. MR images at the age of 3 weeks.

A, Axial fast spin-echo T2-weighted MR image (3500/90/1) shows high signal intensity in the posterior limbs of the internal capsules suggesting abnormal myelin.

B, Diffusion-weighted MR image demonstrates high signal intensity in the posterior limb of the internal capsule.

C, ADC map corresponding to area in panel *B* shows decreased ADC values in these areas consistent with restricted diffusion.

D, Color-coded fractional anisotropy-map demonstrates preservation of fractional anisotropy in white matter tracts. Red refers to FA = 1 and purple to FA = 0.

values (Fig 1C), consistent with restricted diffusion. On DTI, though, a normal degree of anisotropy was found, which indicates axonal integrity (Fig 1D). Corpus callosum measurements were well below normal, the genu measuring 2.2, the corpus 1.5, and the splenium 2.5 mm.⁶ When the patient was 3 months of age, the axial T2-weighted images showed high signal intensity in anterior and posterior limbs of the internal capsules, optic radiations, ventral brain stem, central cerebellar white matter, and in the peripheral white matter of the corona radiata and centrum semiovale (Fig 2A). DWIs showed high signal intensity (Fig 2B) and low ADC (Fig 2C) in these regions, consistent with restricted diffusion in areas where myelin is normally present. DTI showed age-related increase in fractional anisotropy in the cerebral white matter tracts.

MR imaging performed at 17 months showed moderate cerebral atrophy. Interestingly, the high signal intensity on DWI had disappeared (Fig 3A). The fractional anisotropy maps showed decreased anisotropy throughout the brain (Fig 3B).

Discussion

Inherent to the generally fulminant course of classical NKH most neuropathologic data in NKH are referred to neonates.⁷⁻¹¹ Neuropathologic findings related to myelin in NKH consist of spongy myelinopathy in myelinated ar-

eas.^{9,10} Vacuoles result from intra-period myelin splitting.¹⁰ Microcystic changes were mostly found in the ascending tracts in the brain stem, posterior limbs of the internal capsules, the cerebellar peduncles, optic tracts, and optic chiasm. Areas that myelinate later in life, like the peripheral white matter in the centrum semiovale, corona radiata, and corticospinal tracts show no or mild spongiotic changes. Electron microscopic studies have located the microcysts within the myelin sheaths, splitting the myelin at the intraperiod lines, without axonal changes.^{8,10} Only mild gliosis and few macrophages are found in the spongiotic white matter.⁸⁻¹⁰ Some authors concluded retarded myelination of white matter,^{8,9,11} but others found the stage of myelination to be normal.^{7,10}

Reported autopsies with survival of 15,¹² 24, and 36 months¹³ described cortical atrophy, white matter degeneration, thin corpus callosum, and cerebellar atrophy, with variable degrees of gliosis. The diameters of many of the vacuoles shown in figures in the report by Shuman et al appear to be several times the nuclear diameters.¹³ In neonatal autopsies these vacuoles were much smaller, with diameters less than the axon diameter size and at most equal to the nuclear diameters.^{8,10}

MR imaging findings of increased signal intensity on DWI, together with lowered ADC values in previous studies,^{4,5} reflect the neuropathology reports. Our DWI/ADC findings are similar to the previous studies. We applied DTI to the long-term follow-up of a single patient to obtain an integrated pattern of the impact on both myelin and axons. Our findings at 3 weeks of age were comparable to those of Khong et al⁴ and Sener,⁵ showing increased signal intensity with restricted diffusion of fast myelinating areas. We also observed an increase of the areas with restricted diffusion in the same topographical pattern as seen in normal myelination at 3 months. Thus, myelination itself did not appear to be delayed. On the basis of the DTI there appears to be a high grade of axonal integrity at 3 months, which was subsequently lost as seen upon follow-up at 17 months, shortly before the patient died.

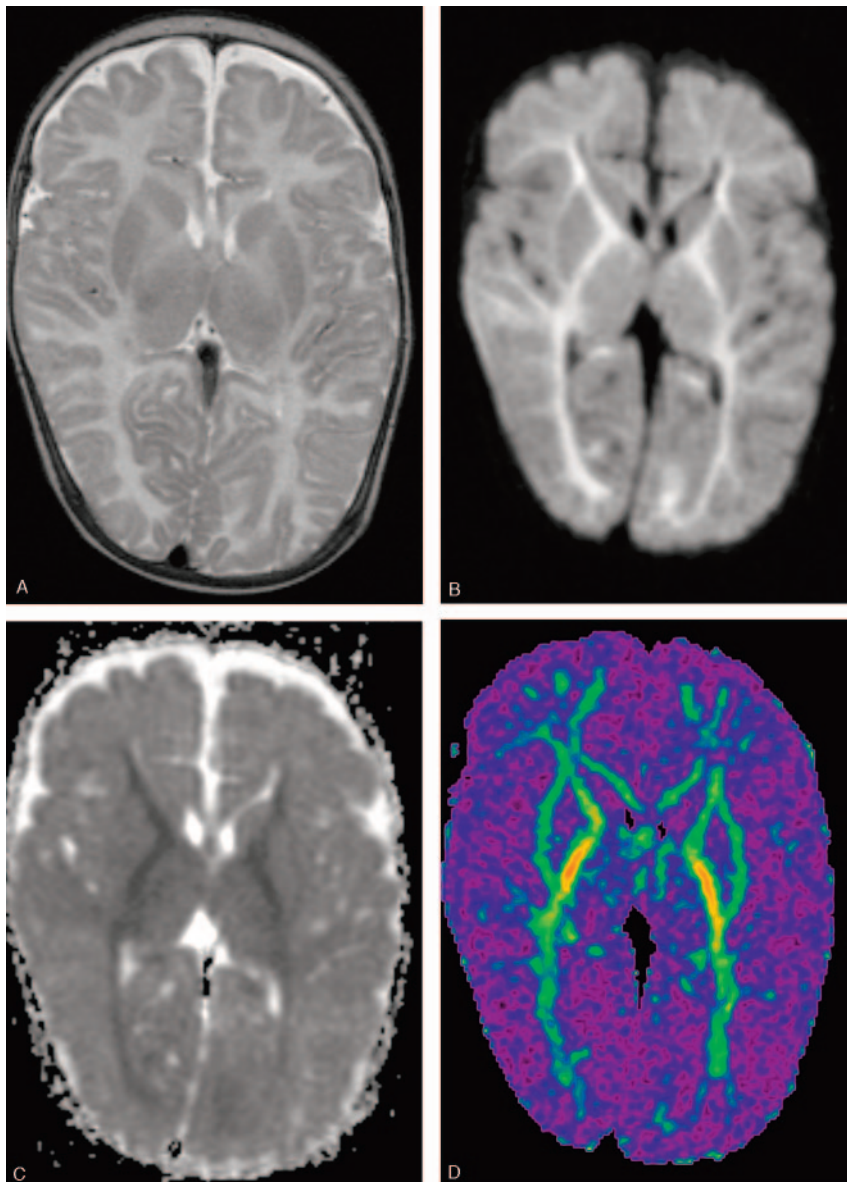


Fig 2. MR images at the age of 3 months.

A, Axial fast spin-echo T2-weighted MR image (3500/90/1) shows high signal intensity in the entire internal capsules and the optic radiations.

B, Diffusion-weighted MR image shows increased signal intensity in the areas indicated in panel *A* and to a lesser degree throughout the white matter.

C, ADC map corresponding to area in panel *B* shows decreased ADC values consistent with restricted diffusion.

D, Color-coded fractional anisotropy map demonstrates preservation of FA in white matter tracts, and increase in FA as compared with Fig 1*D*.

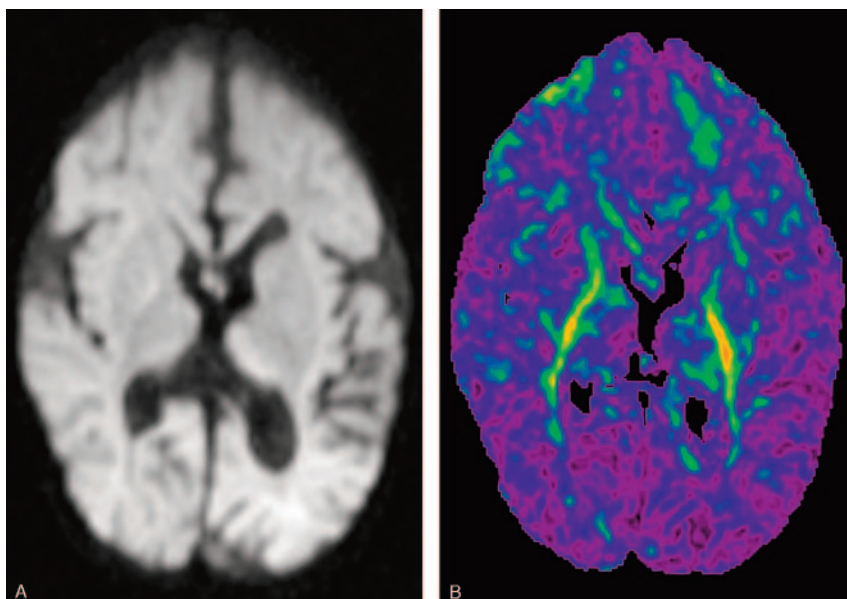


Fig 3. MR images at the age of 17 months.

A, Diffusion-weighted MR image shows atrophy and disappearance of diffusion restriction in the bilateral internal capsules and optic radiations.

B, Color-coded FA map demonstrates FA decrease compared with Fig 2*D*, indicative of axonal loss.

Moseley et al¹⁴ calculated that proton diffusion in any direction is restricted when the axis is $<14\text{--}16\text{ }\mu\text{m}$. Pathologic findings in NKH consist mainly of white matter spongiosis with microcysts, with diameters in the order of $15\text{--}20\text{ }\mu\text{m}$, between the myelin sheaths. It is therefore likely that these microcysts are the cause of diffusion restriction in NKH as suggested elsewhere.^{4,5} Similar findings with restricted diffusion were demonstrated in other diseases with spongiotic changes due to microvacuole formation, such as Canavan disease,¹⁵ Creutzfeldt-Jakob disease,¹⁶ and van der Knaap vacuolating leukoencephalopathy.¹⁷ In our patient with NKH, the disappearance of diffusion restriction at 17 months suggests coalescence of microvacuoles to larger cysts, and the decrease of fractional anisotropy suggests axonal degeneration. These results are consistent with previous neuropathologic findings.^{12,13}

In conclusion, DWI and DTI are valuable techniques for the detection and characterization of white matter tract abnormalities and for following the evolution of the brain pathology in NKH patients.

Acknowledgments

We thank Marie Odile Rolland, Hôpital Debrousse, Lyon, France, for determination of the glycine cleavage system activity in biopsied liver tissue.

References

1. Hamosh A, Johnston MV. **Nonketotic hyperglycinemia**. In: Scriver C, Beaudet A, Valle D, et al, eds. *The metabolic and molecular bases of inherited disease*. 8th ed. New York: McGraw-Hill;2001:2065–78

2. Applegarth DA, Toone JR. **Nonketotic hyperglycinemia (glycine encephalopathy): laboratory diagnosis**. *Mol Genet Metab* 2001;74:139–46
3. Press GA, Barshop BA, Haas RH, et al. **Abnormalities of the brain in nonketotic hyperglycinemia: MR manifestations**. *AJNR Am J Neuroradiol* 1989;10:315–21
4. Khong PL, Lam BC, Chung BH, et al. **Diffusion-weighted MR imaging in neonatal nonketotic hyperglycinemia**. *AJNR Am J Neuroradiol* 2003;24:1181–83
5. Sener RN. **Nonketotic hyperglycinemia: diffusion magnetic resonance imaging findings**. *J Comput Assist Tomogr* 2003;27:538–40
6. Akkerman EM. **Efficient measurement and calculation of MR diffusion anisotropy images using the Platonic variance method**. *Magn Reson Med* 2003;49:599–604
7. Dalla BB, Aicardi J, Goutieres F, et al. **Glycine encephalopathy**. *Neuropediatrics* 1979;10:209–25
8. Brun A, Borjeson M, Hultberg B, et al. **Neonatal non-ketotic hyperglycinemia: a clinical, biochemical and neuropathological study including electronmicroscopic findings**. *Neuropediatrics* 1979;10:195–205
9. Slager UT, Berggren RL, Marubayashi S. **Nonketotic hyperglycinemia: report of a case and review of the clinical, chemical and pathological changes**. *Ann Neurol* 1977;1:399–402
10. Agamanolis DP, Potter JL, Herrick MK, et al. **The neuropathology of glycine encephalopathy: a report of five cases with immunohistochemical and ultrastructural observations**. *Neurology* 1982;32:975–85
11. Bachmann C, Mihatsch MJ, Baumgartner RE, et al. **Non-ketotic hyperglycinemia: peracute course in neonatal period**. *Helv Paediatr Acta* 1971;26:228–43
12. Trauner DA, Page T, Greco C, et al. **Progressive neurodegenerative disorder in a patient with nonketotic hyperglycinemia**. *J Pediatr* 1981;98:272–75
13. Shuman RM, Leech RW, Scott CR. **The neuropathology of the nonketotic and ketotic hyperglycinemias: three cases**. *Neurology* 1978;28:139–46
14. Moseley ME, Cohen Y, Mintorovitch J, et al. **Early detection of regional cerebral ischemia in cats: comparison of diffusion- and T2-weighted MRI and spectroscopy**. *Magn Reson Med* 1990;14:330–46
15. Engelbrecht V, Scherer A, Rassek M, et al. **Diffusion-weighted MR imaging in the brain in children: findings in the normal brain and in the brain with white matter diseases**. *Radiology* 2002;222:410–18
16. Mittal S, Farmer P, Kalina P, et al. **Correlation of diffusion-weighted magnetic resonance imaging with neuropathology in Creutzfeldt-Jakob disease**. *Arch Neurol* 2002;59:128–34
17. Gelat F, Calli C, Apaydin M, et al. **Van der Knaap's leukoencephalopathy: report of five new cases with emphasis on diffusion-weighted MRI findings**. *Neuroradiology* 2002;44:625–30